The ionic structure and the electronic states of liquid Li-Pb alloys obtained from *ab initio* molecular dynamics simulations

2000 J. Phys.: Condens. Matter 12 6101

(http://iopscience.iop.org/0953-8984/12/28/307)

J. Phys.: Condens. Matter **12** (2000) 6101–6112. Printed in the UK PII: S0953-8984(00)13593-3

The ionic structure and the electronic states of liquid Li–Pb alloys obtained from *ab initio* molecular dynamics simulations

Y Senda†, F Shimojo and K Hoshino

Faculty of Integrated Arts and Sciences, Hiroshima University, Higashi-Hiroshima 739-8521, Japan

Received 28 April 2000

Abstract. *Ab initio* molecular dynamics simulations are carried out for liquid $Li_{0.8}Pb_{0.2}$ and $Li_{0.5}Pb_{0.5}$ alloys to investigate the ionic structure and the electronic states. In our simulation, the existence of the 'chemical complex' Li_4Pb is not found; rather, a salt-like ordering of Pb ions is seen in the liquid $Li_{0.8}Pb_{0.2}$ alloy. It is found from the calculated partial and total structure factors that this ordering leads to the characteristic behaviour of the total structure factor, which agrees well with the results of a neutron diffraction experiment. The composition dependence of the electronic states is explained on the basis of the ionic configuration. The tendency towards ionicity or charge transfer is seen in both liquid alloys, though the valence-electronic charge distribution is not so localized around the ions.

1. Introduction

Among the liquid alkali–Pb alloys which are well known as compound-forming liquid alloys, the liquid Li–Pb alloys are constituted from the smallest alkali atoms and Pb atoms. The liquid Li–Pb alloys show characteristic behaviours near the 'stoichiometric' composition of Li_4Pb as regards structural, thermal and electrical properties. At this composition the stability function has a strong peak, indicating strongly reduced concentration fluctuations [1], and the entropy of mixing seems to have a dip [2]. The excess volume per atom is negative with a strongest relative deviation of about -18% near the composition of Li_4Pb [3]. At the same composition the thermopower changes its sign and the electrical resistivity peaks at about 500 $\mu\Omega$ cm but still remains metallic [4]. These phenomena have been thought to be associated with a charge transfer from alkali atoms to Pb atoms, due to the large difference in electronegativity between alkali and Pb atoms.

The large-alkali (K, Rb, Cs)–Pb systems have highly stable crystalline compounds at the equiatomic composition and their ionic structures have tetrahedral Pb_4^{4-} polyanions, so-called 'Zintl ions', separated from each other by the alkali atoms. On the other hand, there is no tetrahedral Pb_4^{4-} polyanion in the LiPb crystalline compound, and a number of more stable compounds are seen around 20% Pb concentration. The common feature of these Li–Pb compounds is that each Pb atom is surrounded by Li atoms only. In the liquid states, it is known from neutron diffraction experiments [5] that the tendency towards hetero-coordination characteristic of such crystalline compounds is most pronounced at $Li_{0.8}Pb_{0.2}$ and that such a hetero-coordination is associated with a 'partially' salt-like bonding between unlike atoms.

† Present address: Department of Computational Science, Faculty of Science, Kanazawa University, Kakuma-machi, Kanazawa 920-1192, Japan

0953-8984/00/286101+12$30.00

To explain the observed phenomena at the composition $Li_{0.8}Pb_{0.2}$, theoretical studies have been carried out extensively and a variety of models for this liquid alloy have been proposed. On the basis of the assumption of the charge transfer mentioned above, the $Li_{0.8}Pb_{0.2}$ alloy was modelled as an ionic liquid, in which the interionic potentials are described by the screened Coulomb potential with the effective charges of Li and Pb atoms [6]. Hoshino considered the liquid $Li_{0.8}Pb_{0.2}$ alloy as a ternary mixture of Li, Pb and Li_4Pb 'molecules', and showed that the calculated structure factor could reproduce the characteristic features of the observed one [7]. In these studies, however, the correlation between the ionic structure and the electronic states was not taken into account. Since the value of the experimental resistivity of the liquid $Li_{0.8}Pb_{0.2}$ alloy is still in the metallic region [4], the ion–electron interaction is expected to significantly contribute to the ionic structure.

An *ab initio* molecular dynamics (MD) simulation is a very effective and successful tool for describing liquid alloys in which the correlation between the ionic configuration and the electronic states plays an important role [8, 9]. We have already carried out *ab initio* MD simulations for the liquid Na–Pb and K–Pb alloys to investigate the microscopic structure and electronic states [10,11], the results of which have contributed to a better understanding of these liquid alloys. It has been expected from many experimental and theoretical studies that the tetrahedral Pb_4^{4-} polyanions as seen in the equiatomic crystalline compound will persist even in the liquid Na–Pb and K–Pb alloys. It was shown from our calculations that the ionic structures obtained are far from the perfect tetrahedral Zintl-ion picture. For the liquid equiatomic alloys, the polyanions are connected to each other and a complex structure is formed, while they are seen clearly for liquid alkali-rich alloys. In particular, for the liquid K-rich alloy, tetrahedral Pb_4^{4-} appears as an isolated cluster with a high stability. It is found that the Pb polyanions become more stable with increasing size of the alkali atoms, as was suggested by Geertsma and van der Lugt [12].

Under these circumstances, it is interesting to carry out an *ab initio* MD simulation for the liquid alloy which is constituted from the smallest alkali Li atoms and Pb atoms. In this paper we carry out *ab initio* MD simulations for the liquid $Li_{0.8}Pb_{0.2}$ and $Li_{0.5}Pb_{0.5}$ alloys. The purposes of this paper are (i) to investigate the ionic structures and the electronic states, and the relationship between them, and (ii) to provide a microscopic interpretation for the observed characteristic features such as the composition dependence of the structure and the electrical resistivity.

In section 2 we briefly summarize the method of our *ab initio* MD simulation. In sections 3 and 4, the results of our calculation are given and discussed in comparison with the experiment.

2. Method

To study the structure and the electronic states of liquid Li–Pb alloys, we carry out an *ab initio* MD simulation, which is based on the density functional theory in the local-density approximation, the pseudopotential theory and the adiabatic approximation. We minimize the Kohn–Sham energy functional for a given ionic configuration by the conjugate-gradient method [13, 14] and calculate the electron density and the forces acting on ions on the basis of the Hellmann–Feynman theorem.

We use the norm-conserving pseudopotential proposed by Troullier and Martins [15] for both Li and Pb atoms. The Pb pseudopotential is generated from the scalar-relativistic atomic calculation [16]. The non-local part of the pseudopotential is calculated using the Kleinman–Bylander separable form [17]. The exchange–correlation energy is calculated in the local-density approximation [18,19]. The partial-core correction [20] is taken into account to guarantee the transferability of the pseudopotentials employed. The fractional occupancies

of energy levels are introduced in order to ensure the convergence of the electronic states of the metals. The wavefunction, sampled only at the Γ point of the Brillouin zone, is expanded in plane waves and their cut-off energy is 10 Ryd, which is determined as the value required to achieve convergence of the total energy to within 1 mRyd/electron.

In our calculations, a cubic supercell is used and the periodic boundary condition is imposed. The total number of atoms in the supercell is taken to be one hundred. The side of the cubic cell is about 13–14 Å. As an initial configuration, Li and Pb atoms are randomly arranged on the simple-cubic lattice.

A constant-temperature MD simulation is carried out using the Nosé–Hoover thermostat technique [21, 22]. The classical equations of motion are solved using the velocity Verlet algorithm. Our simulation is carried out for 4.8 ps with the time step of 1.2 fs after the thermal equilibrium state is achieved. The temperatures are 1075 K and 805 K for the liquid $Li_{0.8}Pb_{0.2}$ and $Li_{0.5}Pb_{0.5}$ alloys, respectively. The observed densities [3] are used in our calculation.

3. The structural properties of liquid Li–Pb alloys

3.1. The partial radial distribution functions

The ionic structure of the liquid $Li_{0.8}Pb_{0.2}$ alloy is expected to be reflected by that of the crystalline compound Li_7Pb_2, whose composition is close to that of $Li_{0.8}Pb_{0.2}$. The compound Li_7Pb_2 has a hexagonal structure with nine atoms in the unit cell and there are no Pb–Pb nearest neighbours; each Pb atom is surrounded by Li atoms only. To investigate the chemical short-range order in liquid Li–Pb alloys, we obtained the partial radial distribution functions $g_{\mathrm{LiLi}}(r)$, $g_{\mathrm{LiPb}}(r)$ and $g_{\mathrm{PbPb}}(r)$ from our simulations for the liquid $Li_{0.8}Pb_{0.2}$ alloy. It is seen from figure 1 that the height of the first peak of $g_{\mathrm{LiPb}}(r)$ is relatively large compared with those for $g_{\mathrm{LiLi}}(r)$ and $g_{\mathrm{PbPb}}(r)$. The most characteristic features found in $g_{\mathrm{PbPb}}(r)$ for the liquid $Li_{0.8}Pb_{0.2}$ alloy are the absence of the first peak around the Pb–Pb nearest-neighbour distance 3.2 Å and the anomalously high second peak. The absence of the first peak is consistent with the fact that there are no Pb–Pb nearest neighbours in the corresponding crystal compound. The position of the second peak, 5.1 Å, corresponds to the Pb–Pb distance in the crystalline compound, $d_{\mathrm{Pb-Pb}} = 4.75$ Å. For these reasons, we conclude that the tendency towards hetero-coordination seen in the crystalline compound is also found in the liquid $Li_{0.8}Pb_{0.2}$ alloy.

We also calculated the distribution functions $P(n)$ for the average coordination number of Li atoms around each Pb atom, which are shown in figure 2 for the liquid $Li_{0.8}Pb_{0.2}$ and $Li_{0.5}Pb_{0.5}$ alloys. $P(n)$ is defined as the probability that each Pb atom has n neighbouring Li atoms within the first coordination shell of radius 4 Å. Though $P(4)$ should be large if there exists a chemical complex Li_4Pb, the peak of $P(n)$ appears around $n = 10$–13. Note that, in the present definition of $P(n)$, the first coordination shell overlaps with that of the adjacent Pb atoms and therefore $P(n)$ tends to overestimate its value.

From these results we conclude that the chemical complex Li_4Pb does not exist in the liquid Li–Pb alloys, i.e. the stable chemical bonding between Li and Pb ions within the chemical complex Li_4Pb has not been found in our simulation.

On the other hand, for the liquid $Li_{0.5}Pb_{0.5}$ alloy, the first peak around 3.2 Å clearly appears in the partial radial distribution function $g_{\mathrm{PbPb}}(r)$ as is seen in figure 1; the function has the form of that of an ordinary liquid, which is in contrast to the case for the liquid $Li_{0.8}Pb_{0.2}$ alloy. The position of the first peak $r \simeq 3.25$ Å is consistent with that for pure liquid lead.

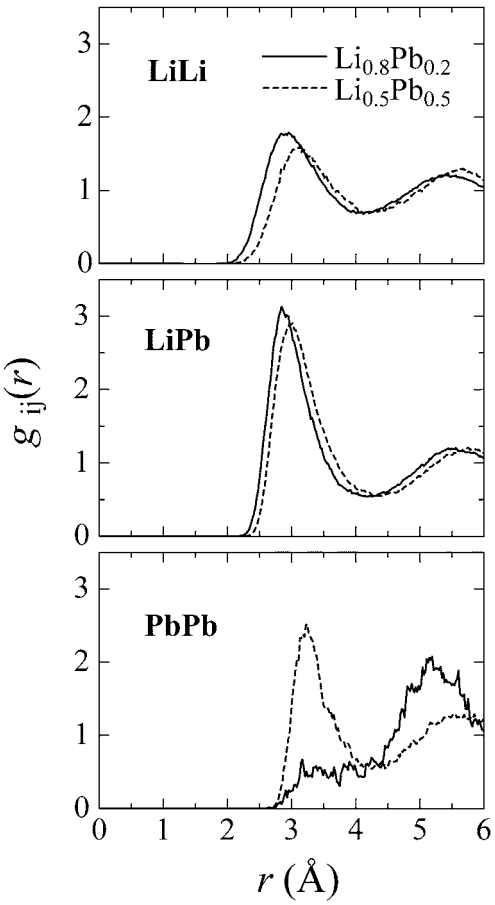

Figure 1. The partial radial distribution functions $g_{\mathrm{LiLi}}(r)$, $g_{\mathrm{LiPb}}(r)$ and $g_{\mathrm{PbPb}}(r)$ for the liquid $Li_{0.8}Pb_{0.2}$ (solid line) and $Li_{0.5}Pb_{0.5}$ (broken line) alloys.

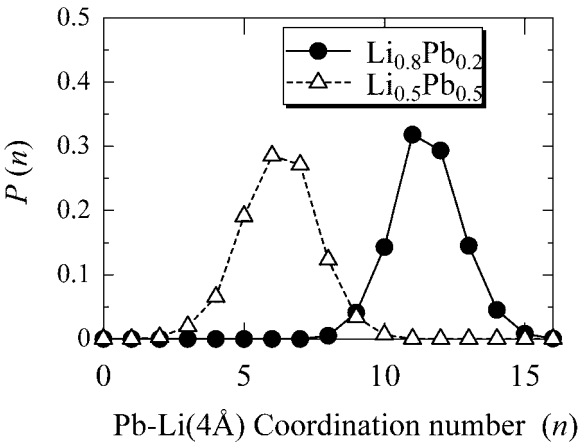

Figure 2. The coordination-number distribution function $P(n)$ of Li ions around a Pb ion for the liquid $Li_{0.8}Pb_{0.2}$ (solid line) and $Li_{0.5}Pb_{0.5}$ (broken line) alloys.

3.2. The partial and the total structure factors

To compare the results of our simulation with the neutron diffraction results, we consider the partial and the total structure factors. The Ashcroft–Langreth (AL) partial structure factors

$S_{ij}(k)$ are defined by

$$S_{ij}(k) = \frac{1}{(N_i N_j)^{1/2}} \left\langle \sum_{\mu=1}^{N_i} \sum_{\nu=1}^{N_j} \mathrm{e}^{\mathrm{i}\boldsymbol{k}\cdot(\boldsymbol{r}_\mu - \boldsymbol{r}_\nu)} \right\rangle \tag{1}$$

where the $\{\boldsymbol{r}_\mu\}$ are the positions of ions obtained by our *ab initio* MD simulations. Here N_i is the number of ions of the ith species and the $\langle \cdots \rangle$ means the time average. In figure 3 the AL partial structure factors thus calculated are shown for the liquid $Li_{0.8}Pb_{0.2}$ and $Li_{0.5}Pb_{0.5}$ alloys.

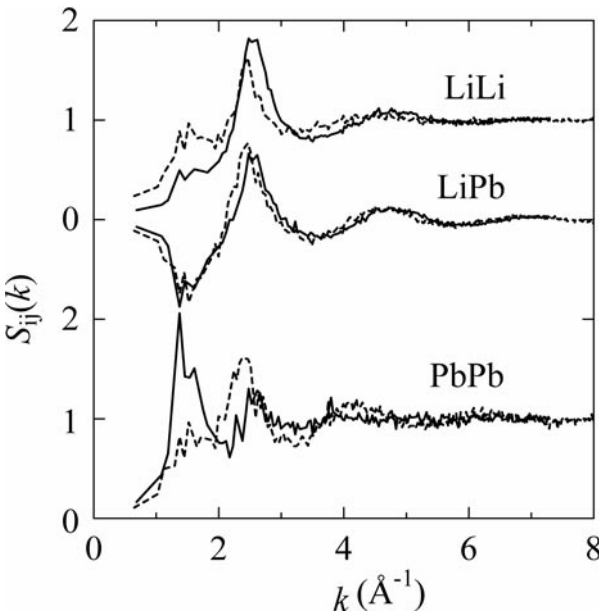

Figure 3. The Ashcroft–Langreth partial structure factors $S_{\mathrm{LiLi}}(k)$, $S_{\mathrm{LiPb}}(k)$ and $S_{\mathrm{PbPb}}(k)$ for the liquid $Li_{0.8}Pb_{0.2}$ (solid line) and $Li_{0.5}Pb_{0.5}$ (broken line) alloys.

The total structure factor $S(k)$ observed in the neutron diffraction experiment is expressed by a linear combination of the partial structure factors $S_{ij}(k)$ as

$$S(k) = \sum_{i,j} (c_i c_j)^{1/2} b_i b_j S_{ij}(k) \Big/ \sum_i c_i b_i^2 \tag{2}$$

where the c_i and b_i are the concentration and the neutron scattering length of the ith species, respectively. For the ^{7}Li isotope, $b_{^7\mathrm{Li}} = -0.22 \times 10^{-12}$ cm and for the natural Pb, $b_{\mathrm{Pb}} = 0.940 \times 10^{-12}$ cm.

In figure 4 we show the calculated total structure factors for the liquid $Li_{0.8}Pb_{0.2}$ and $Li_{0.5}Pb_{0.5}$ alloys, which are compared with the observed structure factors [5]. It is seen that our calculated structure factors are in good agreement with the experimental results. The main peaks around $k \simeq 2.6$ Å^{-1} of $S_{\mathrm{LiLi}}(k)$ and $S_{\mathrm{LiPb}}(k)$ shown in figure 3 do not appear in the total $S(k)$, since the contributions from $S_{\mathrm{LiLi}}(k)$ and $S_{\mathrm{LiPb}}(k)$ to the total $S(k)$ cancel each other, due to the negative scattering length of the ^{7}Li isotope.

Alternatively, we can also express the total structure factor using the Bhatia and Thornton (BT) partial structure factors [23] as

$$S(k) = \bar{b}^2 S_{NN}(k) + (b_{\mathrm{Li}} - b_{\mathrm{Pb}})^2 S_{CC}(k) + 2\bar{b}(b_{\mathrm{Li}} - b_{\mathrm{Pb}}) S_{NC}(k)/(c_{\mathrm{Li}} b_{\mathrm{Li}}^2 + c_{\mathrm{Pb}} b_{\mathrm{Pb}}^2) \tag{3}$$

where the concentration–concentration structure factor $S_{CC}(k)$, the number–number structure factor $S_{NN}(k)$ and the number–concentration structure factor $S_{NC}(k)$ are related to the AL

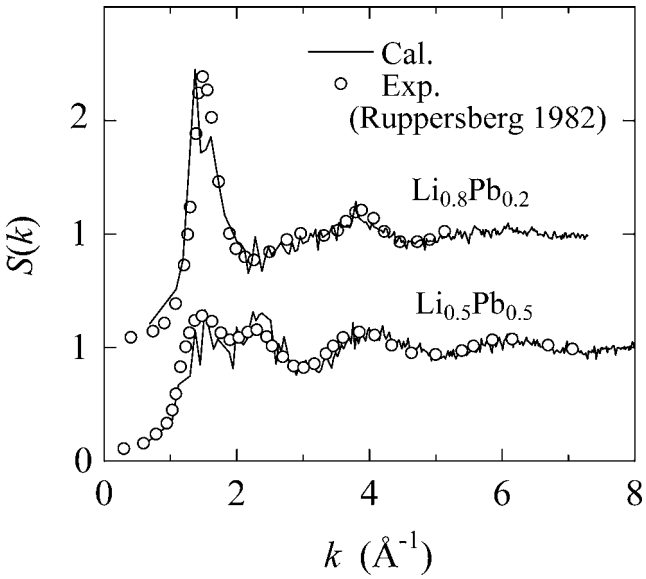

Figure 4. The calculated total structure factors for the liquid $Li_{0.8}Pb_{0.2}$ and $Li_{0.5}Pb_{0.5}$ alloys (open circles). The results of the neutron scattering experiment (solid line) [5] are shown for comparison.

partial structure factors as

$$S_{CC}(k) = c_{\mathrm{Li}}c_{\mathrm{Pb}}(c_{\mathrm{Pb}}S_{\mathrm{LiLi}}(k) + c_{\mathrm{Li}}S_{\mathrm{PbPb}}(k) - 2(c_{\mathrm{Li}}c_{\mathrm{Pb}})^{1/2}S_{\mathrm{LiPb}}(k)) \tag{4}$$

$$S_{NN}(k) = c_{\mathrm{Li}}S_{\mathrm{LiLi}}(k) + c_{\mathrm{Pb}}S_{\mathrm{PbPb}}(k) + 2(c_{\mathrm{Li}}c_{\mathrm{Pb}})^{1/2}S_{\mathrm{LiPb}}(k) \tag{5}$$

and

$$S_{NC}(k) = c_{\mathrm{Li}}c_{\mathrm{Pb}}(S_{\mathrm{LiLi}}(k) - S_{\mathrm{PbPb}}(k) + (c_{\mathrm{Pb}} - c_{\mathrm{Li}})S_{\mathrm{LiPb}}(k)/(c_{\mathrm{Li}}c_{\mathrm{Pb}})^{1/2}). \tag{6}$$

In general, we need three independent scattering data to obtain the partial structure factors. It is possible, however, to obtain $S_{CC}(k)$ by a single neutron diffraction experiment for a special case, i.e. for the so-called 'zero alloy'. At the composition of $Li_{0.8}Pb_{0.2}$, since the neutron scattering length for the ^{7}Li isotope is negative, the average value of the scattering length $\bar{b}$ is very close to zero ($\bar{b} = c_{\mathrm{Li}}b_{\mathrm{Li}} + c_{\mathrm{Pb}}b_{\mathrm{Pb}} = 0.04$); for this reason it is called 'a zero alloy'. In this case we can obtain $S_{CC}(k)$ from a single neutron scattering experiment, because the first and the third terms on the right-hand side of equation (3) vanish and, as a result, $S(k)$ is directly proportional to $S_{CC}(k)$. The calculated $S_{CC}(k)$ and $S_{NN}(k)$ are shown in figure 5, in which the position of the main peak of $S_{CC}(k)$ is in a lower k-region than that of $S_{NN}(k)$. This is associated with the tendency towards hetero-coordination, since the position of the first peak of $S_{CC}(k)$ ($S_{NN}(k)$) is related to the reciprocal of the distance between the like (unlike) atoms.

The salt-like ordering of Pb ions of the liquid $Li_{0.8}Pb_{0.2}$ alloy gives rise to the first peak around $k \simeq 1.5$ Å^{-1} of the observed $S(k)$ or $S_{CC}(k)$. This first peak comes from that of $S_{\mathrm{PbPb}}(k)$ shown in figure 3, since $S(k)$ is expressed as the linear combination of the $S_{ij}(k)$. The position of the first peak, $k = 1.5$ Å^{-1}, corresponds to the real-space distance $r = 5.0$ Å, at which the high second peak of $g_{\mathrm{PbPb}}(r)$ exists. The second peak results from the tendency towards hetero-coordination, which is also seen in the crystalline compound Li_7Pb_2 as was previously mentioned. Such an ordering peculiar to an ionic liquid leads to the characteristic behaviour of the observed $S(k)$. For the liquid $Li_{0.5}Pb_{0.5}$ alloy, the existence of Pb–Pb nearest neighbours contributes to the main peak of $S_{\mathrm{PbPb}}(k)$ at $k \simeq 2.5$ Å^{-1} and then to the second peak of $S(k)$.

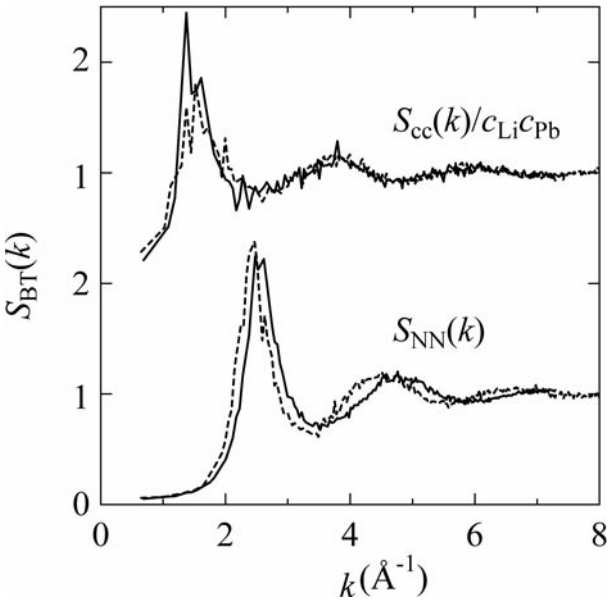

Figure 5. The concentration–concentration structure factors $S_{CC}(k)$ and the number–number structure factors $S_{NN}(k)$ for the liquid $Li_{0.8}Pb_{0.2}$ (solid line) and $Li_{0.5}Pb_{0.5}$ (broken line) alloys.

4. The electronic states of liquid Li–Pb alloys

We show in figure 6 the electrical conductivities as functions of the frequency ($\sigma(\omega)$) calculated using the Kubo–Greenwood formula. The extrapolated values $\sigma(0)$ give the DC conductivities. In figure 7, the calculated resistivities ($=1/\sigma(0)$) of the liquid $Li_{1-x}Pb_x$ alloy are shown as a function of the composition of Pb, x. The observed composition dependence of the resistivity [4] shows the sharp maximum at $Li_{0.8}Pb_{0.2}$, which is reproduced qualitatively as is seen in figure 7. Note that there are some ambiguities in estimating the value of $\sigma(0)$.

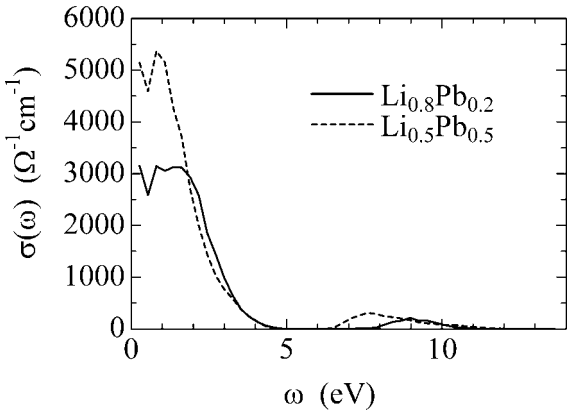

Figure 6. The calculated electrical conductivities $\sigma(\omega)$ as functions of the frequency ω for the liquid $Li_{0.8}Pb_{0.2}$ (solid line) and $Li_{0.5}Pb_{0.5}$ (broken line) alloys.

We show in figures 8 and 9 the total and the partial electronic densities of states (DOS), respectively, which are obtained by sampling 10 k-points of the Brillouin zone and by averaging over some ionic configurations. The lth component of the partial DOS of the ith species is calculated by projecting the wavefunctions on the spherical harmonics within a sphere of radius

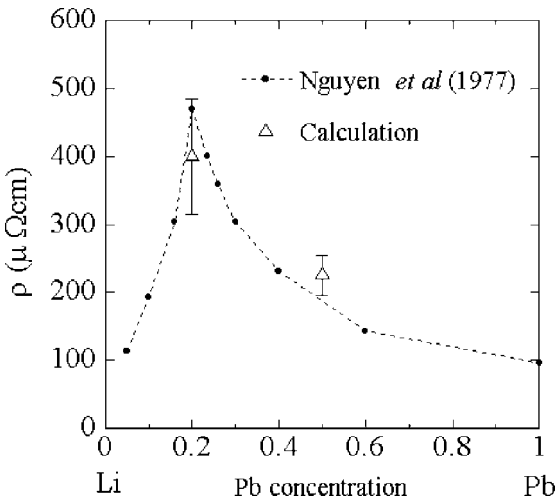

Figure 7. The calculated electrical resistivity (triangles) of the liquid $Li_{1-x}Pb_x$ alloy as a function of the composition of Pb, x. The observed resistivities [4] are also shown, by dots.

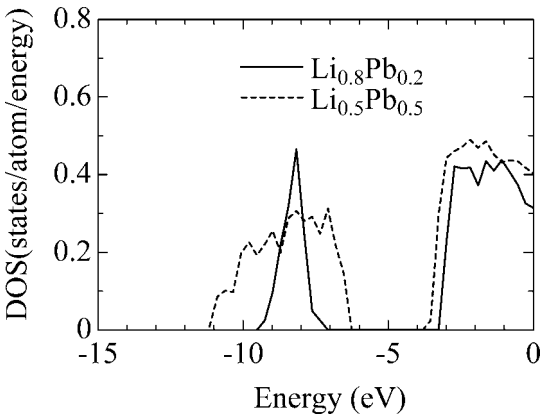

Figure 8. The total densities of states for the liquid $Li_{0.8}Pb_{0.2}$ (solid line) and $Li_{0.5}Pb_{0.5}$ (broken line) alloys. The origin of energy is taken to be the Fermi level.

R_c centred at each μth atom of the ith species, the position of which is $\boldsymbol{r}_\mu$, as

$$D_i^l(\epsilon) = \sum_{\mu=1}^{N_i} \sum_{\alpha} \sum_{m=-l}^{l} \int_0^{R_c} |\boldsymbol{r} - \boldsymbol{r}_\mu|^2 \, \mathrm{d}|\boldsymbol{r} - \boldsymbol{r}_\mu| \left| \int Y_{lm}^*(\Omega_\mu) \psi_\alpha(\boldsymbol{r}) \, \mathrm{d}\Omega_\mu \right|^2 \delta(\epsilon - \epsilon_\alpha) \Big/ N_i \quad (7)$$

where N_i is the number of ions of the ith species, $\psi_\alpha(\boldsymbol{r})$ is the wavefunction of αth state with the eigenvalue ϵ_α and $Y_{lm}(\Omega_\mu)$ is the spherical harmonic with the angular momentum l, which is centred at the μth ion. R_c is chosen to be about half of the average nearest-neighbour distance, on which the partial DOS does not depend significantly. The origin of the energy is taken to be the Fermi level.

The band ranging from -11 eV to -6 eV, which comes from the Pb 6s states, becomes wider with increasing number of Pb atoms. This is simply explained by associating it with the ionic structure: the existence of Pb–Pb nearest neighbours in the liquid $Li_{0.5}Pb_{0.5}$ alloy leads to the increasing overlap of the wavefunction of Pb 6s states, and gives rise to the wider energy band. The hybridization of the Pb 6p states and the Li 2s states is seen around the Fermi level, where the characteristic behaviour is found for the partial DOS of the Pb atom, i.e. the considerable decrease of the electronic states for the $Li_{0.8}Pb_{0.2}$ alloy.

Because of the large difference in electronegativity between Li and Pb atoms (the electronegativity on Pauling's scale is 0.98 for the Li atom and 2.33 for the Pb atom), their mixture has

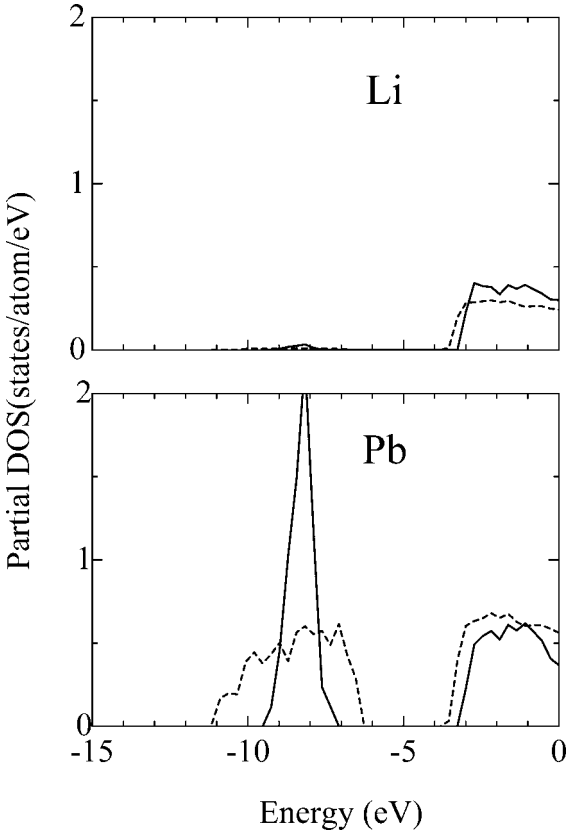

Figure 9. The partial densities of states for the liquid $Li_{0.8}Pb_{0.2}$ (solid line) and $Li_{0.5}Pb_{0.5}$ (broken line) alloys. The origin of energy is taken to be the Fermi level.

been expected to have an ionic character, i.e. some degree of electronic charge transfer from Li atoms to Pb atoms. As is shown in figure 7, the observed resistivity shows anomalous behaviour at the 'stoichiometric' composition of $Li_{0.8}Pb_{0.2}$, which is considered to be the most favourable composition for the ionicity from the point of view of achieving a complete electron transfer and construction of the closed shell of the Pb atom. We investigate the ionicity of the liquid as follows: figure 10 shows the 'difference' of the electron-density distribution $\rho(\boldsymbol{r})$ for the ionic configuration of the liquid $Li_{0.8}Pb_{0.2}$ alloy from the electron-density distribution obtained by the linear combination of the atomic valence-electron-density distribution $\rho_{\mathrm{atom}}(\boldsymbol{r})$, calculated from

$$\Delta\rho(\boldsymbol{r}) = \rho(\boldsymbol{r}) - \sum_{\mu} \rho_{\mathrm{atom}}(|\boldsymbol{r} - \boldsymbol{r}_{\mu}|) \tag{8}$$

where $\boldsymbol{r}_{\mu}$ is the position of the μth atom of the corresponding ionic configuration shown in figure 10. The blue region means $\Delta\rho(\boldsymbol{r}) < 0$ and the red one means $\Delta\rho(\boldsymbol{r}) > 0$. When the ions are on the plane where the electron-density distribution is calculated, the core regions are shown by black holes since $\Delta\rho(\boldsymbol{r}) < 0$ and $|\Delta\rho(\boldsymbol{r})| \ll \rho_0$ in those regions, ρ_0 being the average electron density. It is seen that the regions around Li ions are dominated by the blue region, while those around Pb ions are dominated by the red region. This means that the charge transfer occurs from Li atoms to Pb atoms. Such a salt-like bonding between Li and Pb ions is closely related to the ionic hetero-coordination of the liquid Li–Pb alloy [5].

However, the purely ionic description for the liquid $Li_{0.8}Pb_{0.2}$ alloy is an over-simplification: its character is in between the character of a liquid metal and that of an ionic

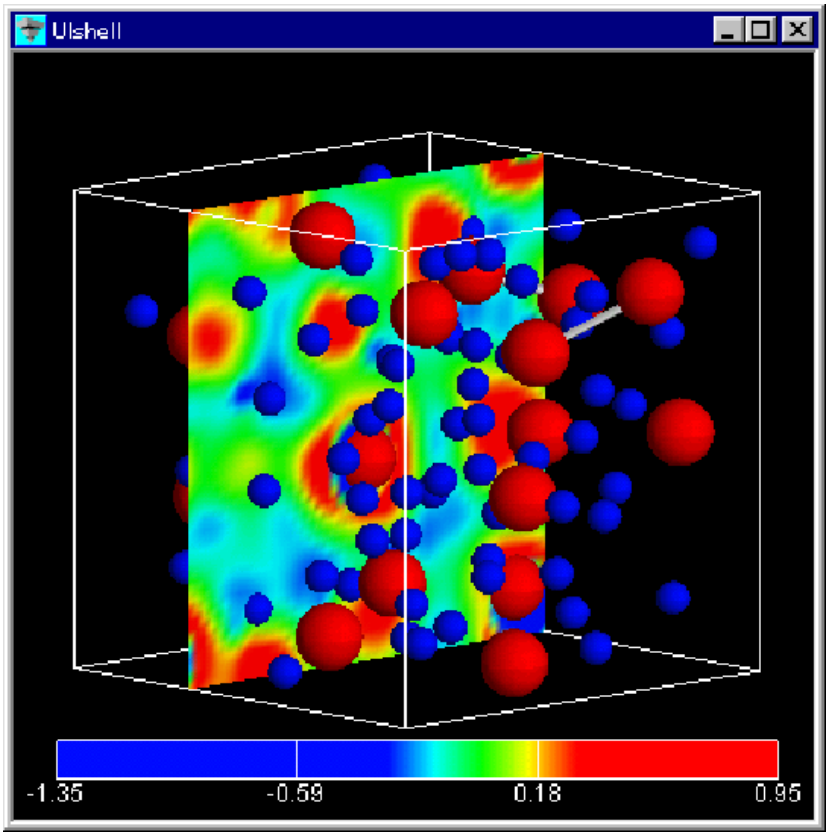

Figure 10. The difference of the electron-density distribution for the ionic configuration of the liquid $Li_{0.8}Pb_{0.2}$ alloy from the linear combination of the atomic valence-electron-density distribution. The Li and Pb ions are drawn as blue and red balls, respectively.

liquid. In fact, the value of the observed resistivity ($\rho = 470\ \mu\Omega$ cm) for the liquid $Li_{0.8}Pb_{0.2}$ alloy is in the metallic region. It is understood from our electronic structure calculations that the charge transfer from Li to Pb atoms is not so large as is seen from the occupied partial DOS of the Li atom shown in figure 9. The electron-density distribution obtained by the present calculation indicates that a considerable number of valence electrons remain around Li ions. It may be said at least that Li atoms 'partially' transfer their valence electrons to Pb atoms.

We now consider why the maximum of the electrical resistivity appears at the composition $Li_{0.8}Pb_{0.2}$. The quantitative estimation of the electronic charge transfer cannot be well defined, since the electronic charge is not well localized around the ions and rather spreads spatially. We focus on the behaviour of the wavefunction near the Fermi level, since the electronic states near the Fermi level give the main contribution to the conductivity. The electronic charge density calculated from the wavefunctions near the Fermi level is defined as

$$\rho_0(\boldsymbol{r}) = \sum_{\alpha}{}' \psi_\alpha^*(\boldsymbol{r})\psi_\alpha(\boldsymbol{r}) \tag{9}$$

where $\sum'_\alpha$ means that the summation of the states α is taken over ten states below the Fermi level. We show in figures 11(a) and 11(b) thus-defined electronic charge distributions for the liquid $Li_{0.8}Pb_{0.2}$ and $Li_{0.5}Pb_{0.5}$ alloys, respectively. It is seen from this figure that the

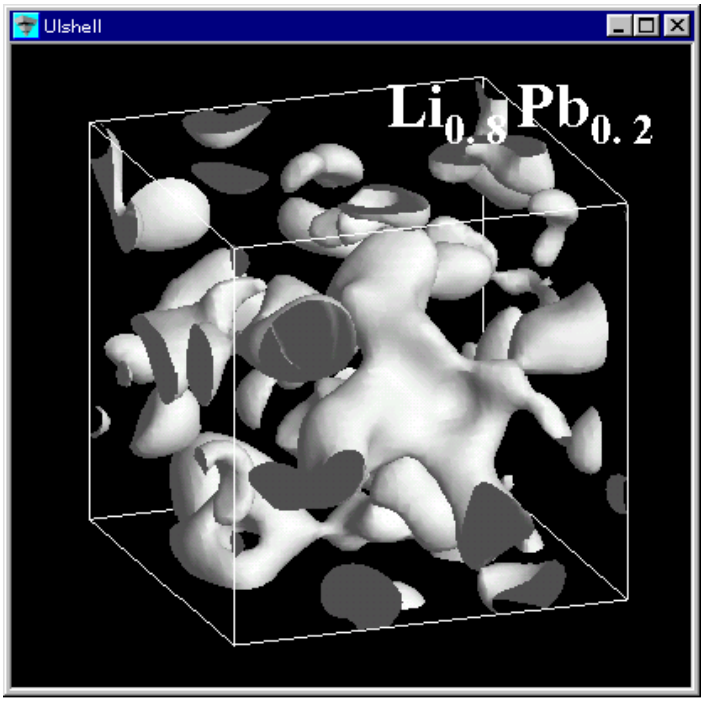

(a)

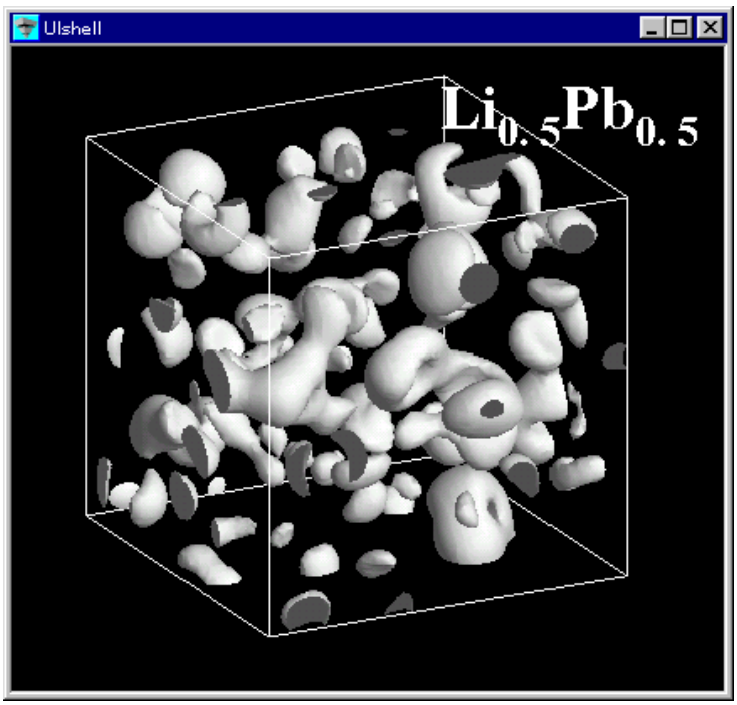

(b)

Figure 11. The electronic charge-density distribution calculated from the wavefunctions near the Fermi level for the liquid (a) $Li_{0.8}Pb_{0.2}$ and (b) $Li_{0.5}Pb_{0.5}$ alloys.

wavefunction for the liquid $Li_{0.8}Pb_{0.2}$ alloy is more localized than that for the liquid $Li_{0.5}Pb_{0.5}$ alloy. We conclude that the maximum of the resistivity at the composition of $Li_{0.8}Pb_{0.2}$ is closely related to the localization of the wavefunction as well as the decrease in the number of electronic states around the Fermi level.

5. Summary

We have carried out *ab initio* molecular dynamics simulations for liquid $Li_{0.8}Pb_{0.2}$ and $Li_{0.5}Pb_{0.5}$ alloys in order to investigate the composition dependence of the ionic configuration and the electronic states.

As regards the structural properties, we have clarified that the chemical short-range order observed as the first peak of the total structure factor for the liquid $Li_{0.8}Pb_{0.2}$ alloy comes from charge ordering, which is clearly seen in the concentration–concentration structure factor.

The peak of the observed electrical resistivity at the composition of $Li_{0.8}Pb_{0.2}$ can be understood on the basis of the dip at the Fermi level of the electronic density of states and the localized nature of the wavefunction with the energy eigenvalue near the Fermi level.

Acknowledgments

This work was supported by a Grant-in-Aid for Scientific Research from the Ministry of Education, Science, Sports and Culture, Japan. We acknowledge the Centre for Promotion of Computational Science and Engineering (CCSE) of Japan Atomic Energy Research Institute (JAERI) for the use of the NEC SX-4 and FUJITSU VPP300 supercomputers. We also thank the Computer Centre of Tohoku University for allowing us to use the NEC SX-4 supercomputer.

References

[1] Saboungi M-L, Marr J and Blander M 1978 *J. Chem. Phys.* **68** 1375
[2] Becker W, Schwitzgebel G and Ruppersberg H 1981 *Z. Metallk.* **72** 186
[3] Ruppersberg H and Speicher W 1976 *Z. Naturf.* a **31** 47
[4] Nguyen V and Enderby J E 1977 *Phil. Mag.* **35** 1013
[5] Ruppersberg H and Reiter H 1982 *J. Phys. F: Met. Phys.* **12** 1311
[6] Copestake A P, Evans R, Ruppersberg H and Schirmacher 1983 *J. Phys. F: Met. Phys.* **13** 1993
[7] Hoshino K 1983 *J. Phys. F: Met. Phys.* **13** 1981
[8] Senda Y, Shimojo F and Hoshino K 1998 *J. Phys. Soc. Japan* **67** 916
[9] Senda Y, Shimojo F and Hoshino K 1998 *J. Phys. Soc. Japan* **67** 2753
[10] Senda Y, Shimojo F and Hoshino K 1999 *J. Phys.: Condens. Matter* **11** 2199
[11] Senda Y, Shimojo F and Hoshino K 1999 *J. Phys.: Condens. Matter* **11** 5387
[12] Geertsma W and van der Lugt W 1984 *J. Phys. F: Met. Phys.* **14** 1833
[13] Kresse G and Hafner J 1994 *Phys. Rev.* B **49** 14 251
[14] Shimojo F, Zempo Y, Hoshino K and Watabe M 1995 *Phys. Rev.* B **52** 9320
[15] Troullier N and Martins J L 1991 *Phys. Rev.* B **43** 1993
[16] Wood J H and Boring A M 1978 *Phys. Rev.* B **18** 2701
[17] Kleinman L and Bylander D M 1982 *Phys. Rev. Lett.* **48** 1425
[18] Ceperley D M and Alder B J 1980 *Phys. Rev. Lett.* **45** 566
[19] Perdew J P and Zunger A 1981 *Phys. Rev.* B **23** 5048
[20] Louie S G, Froyen S and Cohen M L 1982 *Phys. Rev.* B **26** 1738
[21] Nosé S 1984 *Mol. Phys.* **52** 255
[22] Hoover W G 1985 *Phys. Rev.* A **31** 1695
[23] Bhatia A B and Thornton D E 1970 *Phys. Rev.* B **2** 3004